Springer

KSME

Journal of Mechanical Science and Technology 29 (7) (2015) 2699~2704
www.springerlink.com/content/1738-494x(Print)/1976-3824(Online)
DOI 10.1007/s12206-015-0517-z

# Dynamics and actuating torque optimization of planar robots †

Vinay Gupta[1,*], Himanshu Chaudhary[2] and Subir K. Saha[1]

[1]*Indian Institute of Technology Delhi, New Delhi-110016, India*
[2]*Malviya National Institute of Technology Jaipur, Rajasthan-302017, India*

(Manuscript Received December 14, 2014; Revised April 9, 2015; Accepted April 28, 2015)

**Abstract**

An optimization methodology is presented for design of serial-chain planar robots for minimizing torque at joints, when its end-effector is supposed to move on a prescribed path. In particular, the end-effector of the robot is allowed to move on a circular path. For the respective joint trajectories, the weighted sum of root mean square (RMS) of the actuating torques is minimized by the mass redistribution of the links. To achieve the goal, the DeNOC (Decoupled natural orthogonal complement) based dynamics was formulated by representing the rigid links as a set of rigidly connected point-masses known as equimomental system. The methodology is illustrated using a planar two-degree-of-freedom (DOF) robot with two revolute joints.

*Keywords*: Dynamics; Equimomental system; Optimization; Robots

## 1. Introduction

Serial-chain robots are widely used industrially due to their versatility. Their design is often based on optimization of kinematic criteria like workspace, singularity, and minimum condition number, or on dynamic criteria like minimum torques, energy, shaking force and shaking moment. The latter problem is found to be more challenging due to the difficulty in mathematical modelling for optimization. In this paper we address the second aspect, where design is based on the minimum joint torque requirements. In Ref. [1], the dynamic quantities of a serial robot such as shaking force, shaking moment and driving torques were minimized by optimally distributing the mass of the links. The required actuator torque of a planar robot for a prescribed task was minimized in Ref. [2]. In Refs. [3-5], the average joint torque and electric input energy were minimized for a serial-chain robotic manipulator for a prescribed end-effector trajectory. In Ref. [6], a solution was proposed for minimizing the input torques of the serial manipulator based on minimum energy control and optimal distribution of the movable masses. The concept of point-masses was addresed in Ref. [7] to see the effect of mass balancing on the actuator torques and consumed energy. In Ref. [8], the concept of equimomental system was applied for the minimization of constraint forces in industrial manipulators by redistributing their link masses.

This paper addresses the above problem by formulating an effective dynamic model and applying it in optimum design. We proposed a methodolgy for minimizing the joint torques for a prescribed circular trajectory of the end-effector. To illustrate the methodology a two-DOF planar robot was considered whose link lengths were choosen based on kinetostatic optimization, as proposed in Ref. [9]. The dynamic performance of the kinetostatically optimized robot was not addressed in Ref. [9]. The results aid in deciding the dynamic parameters to minimize the joint torque. For the calculation of joint torque, DeNOC [10] based dynamics was used with the concept of equimomental system of point-masses [11]. Two systems are said to be equimomental if they have the same mass, same mass center location, and same moment of inertia with respect to a common reference frame [12]. The concept of equimomental system is also referred to as point-mass system. It is used as a convenient way of representing the inertial properties which greatly influence the joint torque. Application of this concept in balancing of closed-loop mechanisms is well adressed in Refs. [13, 14].

The paper is organized as follows: Sec. 2 presents the modelling and inverse kinematics of a two-link robot. Sec. 3 derives the inverse dynamics of the robot. Sec. 4 presents the optimization scheme with numerical example, where Sec. 5 discusses the results. Finally, Sec. 6 concludes the paper.

## 2. Modelling and inverse Kinematics

This section describes a two-link robot arm and its inverse

*Corresponding author. Tel.: +91 9212758512, Fax.: +91 11 26582053
E-mail address: vinayguptaiec@gmail.com
† This paper was presented at the Joint Conference of the 3rd IMSD and the 7th ACMD, Busan, Korea, June, 2014. Recommended by Guest Editor Sung-Soo Kim and Jin Hwan Choi

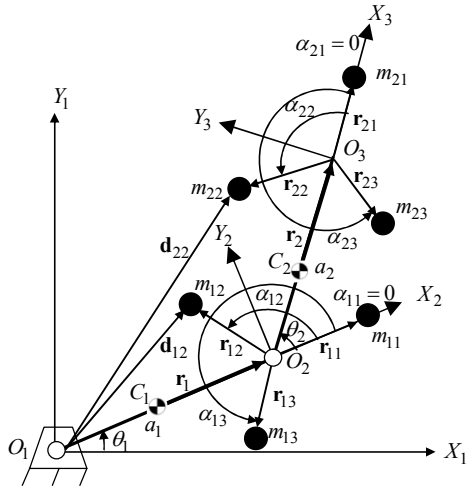


Fig. 1. A Two-link robot with three point-mass model.

kinematics. The results of inverse kinematics are required as inputs to the dynamic model for the calculation of joint torques.

### *2.1 Modelling as equimomental system*

Fig. 1 shows the schematic representation of a planar two-link robot with revolute joints. The mass of each link is denoted by $m_i$, and link length by $a_i$. The angle $\theta_i$ denotes the relative joint angle, the vector $\mathbf{r}_i$ denotes the location of the center of mass $C_i$ from the origin of the body-fixed frame $O_{i+1}$. Each link is represented by its equimomemtal system of three point-masses $m_{ij}$ ($i$ = 1,2 and $j$ = 1,2,3), which are rigidly connected to the body-fixed frame of each link at $O_{i+1}$.

The vector $\mathbf{r}_{ij}$ defines the position of the point-masses from the origin of the body-fixed frame. For the conversion of a continuous rigid body into an equimomental system of point-masses, refer to Ref. [13].

### *2.2 Inverse kinematics*

In this section, inverse kinematics is performed to find the joints trajectories for a prescribed circular trajectory of the end-effector. The circle of radius $l$ is assumed to be traced by the end-effector of a robot with constant angular velocity in time $T$. The coordinate of the end-effector in terms of the center of the circle and its radius is given as

$$x = u + l\cos(2\pi t / T), \tag{1a}$$
$$y = v + l\sin(2\pi t / T), \tag{1b}$$

where $u$ and $v$ are the coordinates of the center of the circle. The joint angles are calculated using Eqs. (1a) and (1b).

$$\theta_1 = \alpha_1; \theta_2 = \alpha_2 - \alpha_1, \tag{2a}$$

where the terms $\alpha_1$ and $\alpha_2$ are as follows:

$$\alpha_1 = \tan^{-1}[(y - a_2\sin(\alpha_2))/(x - a_2\cos(\alpha_2))], \tag{2b}$$
$$\alpha_2 = 2\tan^{-1}\left[-B \pm \sqrt{B^2 + A^2 - C^2}/(C - A)\right]. \tag{2c}$$

In Eqs. (2b) and (2c), $A \equiv 2a_2x$; $B \equiv 2a_2y$; $C \equiv [(a_1^2 + a_2^2 - x^2 - y^2)]$. The corresponding joint velocity and acceleration needed for inverse dynamics are then evaluated by using the concept of Jacobian reported in Ref. [15]. The joint velocities are derived as

$$\begin{bmatrix}\dot{\theta}_1\\ \dot{\theta}_2\end{bmatrix} = \mathbf{J}^{-1}\begin{bmatrix}\dot{x}\\ \dot{y}\end{bmatrix}, \tag{3}$$

where J is the 2 × 2 Jacobian matrix, and given by

$$\mathbf{J} \equiv \begin{bmatrix}-a_1\sin\theta_1 - a_2\sin(\theta_1+\theta_2) & -a_2\sin(\theta_1+\theta_2)\\ a_1\cos\theta_1 + a_2\cos(\theta_1+\theta_2) & a_2\cos(\theta_1+\theta_2)\end{bmatrix}. \tag{4}$$

The components of the input end-effector velocity are as follows,

$$\dot{x} = -l(2\pi/T)\sin(2\pi t/T), \tag{5a}$$
$$\dot{y} = l(2\pi/T)\cos(2\pi t/T). \tag{5b}$$

Furthermore, the joint accelerations are calculated as

$$\begin{bmatrix}\ddot{\theta}_1\\ \ddot{\theta}_2\end{bmatrix} = \mathbf{J}^{-1}\begin{bmatrix}\ddot{x}\\ \ddot{y}\end{bmatrix} - \mathbf{J}^{-1}\dot{\mathbf{J}}\begin{bmatrix}\dot{\theta}_1\\ \dot{\theta}_2\end{bmatrix}, \tag{6}$$

$$\dot{\mathbf{J}} \equiv \begin{bmatrix}-\dot{\theta}a_1\cos\theta_1 - (\dot{\theta}_1+\dot{\theta}_2)a_2\cos(\theta_1+\theta_2) & -(\dot{\theta}_1+\dot{\theta}_2)a_2\cos(\theta_1+\theta_2)\\ -\dot{\theta}a_1\sin\theta_1 - (\dot{\theta}_1+\dot{\theta}_2)a_2\sin(\theta_1+\theta_2) & -(\dot{\theta}_1+\dot{\theta}_2)a_2\sin(\theta_1+\theta_2)\end{bmatrix}, \tag{7}$$

$$\ddot{x} = -l(2\pi/T)^2\cos(2\pi t/T), \tag{8a}$$
$$\ddot{y} = -l(2\pi/T)^2\sin(2\pi t/T). \tag{8b}$$

## 3. Inverse dynamics of two-link robot

In this section, inverse dynamics algorithm of a two-link planar robot arm is presented, which will be used to find its joint torque.

### *3.1 The DeNOC matrices for the point-masses*

Referring to Fig. 1, the DeNOC matrices for the robot arm are derived first. The velocity of each point-mass is given by

$$\mathbf{v}_{ij} = \mathbf{v}_i + \boldsymbol{\omega}_i \times \mathbf{d}_{ij}; \text{for } i = 1,2 \text{ and } j = 1,2,3, \tag{9}$$

where $\boldsymbol{\omega}_i$ and $\mathbf{v}_i$ are the angular velocity and linear velocity of the origin of the respective link, whereas vector $\mathbf{d}_{ij} \equiv \mathbf{a}_i + \mathbf{r}_{ij}$ denotes the position of point-mass from the origin of the respective links. The vector $\mathbf{a}_i$ denotes the position of the origin of the body-fixed frame attached to the body, whereas

the vector $\mathbf{r}_{ij}$ ($i$ = 1, 2 and $j$ = 1, 2, 3) denotes the location of each point-mass from the origin of body-fixed frame. For a system of point-masses, velocities of all the point-masses of the two links can be given from Eq. (9) as

$$\tilde{\mathbf{v}} = \mathbf{D}\mathbf{t}\,, \tag{10}$$

where $\tilde{\mathbf{v}}$ is the 18-dimensional velocity vector, $\mathbf{t}$ is the 12-dimensional vector of twists [10], and $\mathbf{D}$ is the 18 × 12 matrix. Matrix $\mathbf{D}$ and vector $\mathbf{t}$ are defined by

$$\mathbf{D} \equiv \begin{bmatrix} \mathbf{D}_1 & \mathbf{O} \\ \mathbf{O} & \mathbf{D}_2 \end{bmatrix}; \mathbf{t} \equiv \begin{bmatrix} \mathbf{t}_1 \\ \mathbf{t}_2 \end{bmatrix}, \tag{11}$$

where the $9 \times 6$ matrix $\mathbf{D}_i$ and the 6-dimensional $\mathbf{t}_i$ are as follows:

$$\mathbf{D}_i \equiv \begin{bmatrix} -\mathbf{d}_{i1} \times \mathbf{1} & \mathbf{1} \\ -\mathbf{d}_{i2} \times \mathbf{1} & \mathbf{1} \\ -\mathbf{d}_{i3} \times \mathbf{1} & \mathbf{1} \end{bmatrix}; \mathbf{t}_i \equiv \begin{bmatrix} \boldsymbol{\omega}_i \\ \mathbf{v}_i \end{bmatrix}, \text{ for } i = 1,2\,. \tag{12}$$

In Eq. (12), $\mathbf{d}_{ij} \times \mathbf{1}$, for $i$ = 1, 2 and $j$ = 1, 2, 3, is the 3×3 cross-product tensor associated with vector $\mathbf{d}_{ij}$, i.e., $(\mathbf{d}_{ij} \times \mathbf{1})\mathbf{x} = \mathbf{d}_{ij} \times \mathbf{x}$, for any 3-dimensional Cartesian vector $\mathbf{x}$. The term $\mathbf{1}$ is the 3 × 3 identity matrix. For a serial-chain system the twist $\mathbf{t}$ can be expressed in terms of its associated natural orthogonal complement (NOC) or its decoupled form, i.e., the DeNOC [10]. This is given by

$$\mathbf{t} = \mathbf{N}\dot{\boldsymbol{\theta}}, \quad \text{where} \quad \mathbf{N} \equiv \mathbf{N}_l\mathbf{N}_d \text{ and } \dot{\boldsymbol{\theta}} \equiv \left[\dot{\theta}_1, \dot{\theta}_2\right]^T. \tag{13}$$

In Eq. (13), $\mathbf{N}$ is the 12×2 NOC, whereas $\mathbf{N}_l$ and $\mathbf{N}_d$ are the 12×12 and 12×2 matrices, respectively. Combining Eqs. (12) and (13), one can write the point-mass velocities $\tilde{\mathbf{v}}$ in terms of the joint rates, i,e., $\dot{\boldsymbol{\theta}}$, as

$$\tilde{\mathbf{v}} = \tilde{\mathbf{N}}\dot{\boldsymbol{\theta}}, \text{ where } \tilde{\mathbf{N}} \equiv \mathbf{D}\mathbf{N}_l\mathbf{N}_d\,. \tag{14}$$

The matrices $\mathbf{N}_l$ and $\mathbf{N}_d$ of Eq. (14) are given by Ref. [10] as,

$$\mathbf{N}_l \equiv \begin{bmatrix} \mathbf{1} & \mathbf{O} \\ \mathbf{A}_{21} & \mathbf{1} \end{bmatrix}; \text{ and } \mathbf{N}_d \equiv \begin{bmatrix} \mathbf{p}_1 & \mathbf{0} \\ \mathbf{0} & \mathbf{p}_2 \end{bmatrix}, \tag{15}$$

where $\mathbf{O}$ of $\mathbf{N}_l$ is the 6 × 6 matrix of zeros, $\mathbf{0}$ in $\mathbf{N}_d$ is the 6-dimensional vector of zeros, whereas the 6×6 matrix $\mathbf{A}_{21}$ and the 6-dimensional vectors $\mathbf{p}_1$ and $\mathbf{p}_2$ are called the twist propagation matrix and joint-motion propagation vectors, respectively. The 6 × 6 matrix $\mathbf{A}_{21}$ and the 6-dimensional vector $\mathbf{p}_i$ are given by

$$\mathbf{A}_{21} \equiv \begin{bmatrix} \mathbf{1} & \mathbf{O} \\ \mathbf{a}_{21} \times \mathbf{1} & \mathbf{1} \end{bmatrix}; \mathbf{p}_i \equiv \begin{bmatrix} \mathbf{e}_i \\ \mathbf{0} \end{bmatrix} i = 1,2\,, \tag{16}$$

in which $\mathbf{a}_{21} = -\mathbf{a}_1$ is the vector associated to the skew-symmetric matrix $\mathbf{a}_{21} \times \mathbf{1}$. The vector, $\mathbf{e}_i \equiv [0\ 0\ 1]$ is the unit vector parallel to the axis of rotation of each joint.

### *3.2 Equations of motion*

Here the equations of motion are derived to find the joint torque. The equations of motion are derived using the Newton's equation of linear motion and the corresponding DeNOC matrices for the point-masses derived in sub-Sec. 3.1. The unconstrained Newton's equations of linear motion for each point-mass is given as

$$m_{ij}\dot{\mathbf{v}}_{ij} = \mathbf{f}_{ij}, \text{ for i=1,2; } j = 1,2,3\,, \tag{17}$$

where $m_{ij}$ is the mass, $\dot{\mathbf{v}}_{ij}$ is the acceleration and $\mathbf{f}_{ij}$ is the force acting on the respective point-masses of links 1 and 2. Eq. (17) can be written in compact form as

$$\tilde{\mathbf{M}}\dot{\tilde{\mathbf{v}}} = \tilde{\mathbf{f}}\,. \tag{18}$$

In Eq. (18), the 18 × 18 mass matrix $\tilde{\mathbf{M}} \equiv diag.\left[m_{11}\mathbf{1} \quad m_{12}\mathbf{1} \quad m_{13}\mathbf{1} \quad m_{21}\mathbf{1} \quad m_{22}\mathbf{1} \quad m_{23}\mathbf{1}\right]$, the 18-dimensional vectors of velocity and force $\dot{\tilde{\mathbf{v}}}$ and $\tilde{\mathbf{f}}$, respectively, are $\dot{\tilde{\mathbf{v}}} \equiv \left[\dot{\mathbf{v}}_{11}^T \quad \dot{\mathbf{v}}_{12}^T \quad \dot{\mathbf{v}}_{13}^T \quad \dot{\mathbf{v}}_{21}^T \quad \dot{\mathbf{v}}_{22}^T \quad \dot{\mathbf{v}}_{23}^T\right]^T$; $\tilde{\mathbf{f}} \equiv \left[\mathbf{f}_{11}^T \quad \mathbf{f}_{12}^T \quad \mathbf{f}_{13}^T \quad \mathbf{f}_{21}^T \quad \mathbf{f}_{22}^T \quad \mathbf{f}_{23}^T\right]^T$ Now, pre-multiplication of the transpose of $\tilde{\mathbf{N}}$ of Eqs. (14)-(18) leads the minimal set of constrained equations of motion:

$$\tilde{\mathbf{N}}^T\tilde{\mathbf{M}}\dot{\tilde{\mathbf{v}}} = \tilde{\mathbf{N}}^T\tilde{\mathbf{f}}\,, \tag{19}$$

where $\dot{\tilde{\mathbf{v}}} \equiv \tilde{\mathbf{N}}\ddot{\boldsymbol{\theta}} + \dot{\tilde{\mathbf{N}}}\dot{\boldsymbol{\theta}}$. Eq. (19) is the independent set of equations of motion represented as

$$\mathbf{I}\ddot{\boldsymbol{\theta}} + \mathbf{C}\dot{\boldsymbol{\theta}} = \boldsymbol{\tau}\,, \tag{20}$$

in which the $n \times n$ $\mathbf{I}$ is the generalized inertia matrix and $\mathbf{C}$ contains the convective inertia terms. Moreover, $\boldsymbol{\tau}$ is the $n$-dimensional vector of torques. The expressions of $\mathbf{I}$, $\mathbf{C}$ and $\boldsymbol{\tau}$ are given by

$$\mathbf{I} \equiv \tilde{\mathbf{N}}^T\tilde{\mathbf{M}}\tilde{\mathbf{N}};\ \mathbf{C} \equiv \tilde{\mathbf{N}}^T\tilde{\mathbf{M}}\dot{\tilde{\mathbf{N}}};\ \boldsymbol{\tau} = \tilde{\mathbf{N}}^T\tilde{\mathbf{f}}\,. \tag{21}$$

Substituting the corresponding values, the torques can be evaluated recursively as

$$\hat{\mathbf{f}}_2 = \mathbf{D}_2^T\tilde{\mathbf{M}}_2(\dot{\mathbf{D}}_2\mathbf{t}_2 + \mathbf{D}_2\dot{\mathbf{t}}_2); \hat{\mathbf{f}}_1 = \mathbf{D}_1^T\tilde{\mathbf{M}}_1(\dot{\mathbf{D}}_1\mathbf{t}_1 + \mathbf{D}_1\dot{\mathbf{t}}_1) + \mathbf{A}_{21}^T\hat{\mathbf{f}}_2 \tag{22}$$

$$\tau_1 = \mathbf{p}_1^T\hat{\mathbf{f}}_1\,; \tau_2 = \mathbf{p}_2^T\hat{\mathbf{f}}_2\,. \tag{23}$$

## 4. Optimization

In this section, the joint torques are minimized by optimal distribution of the mass of each link. The robot considered is

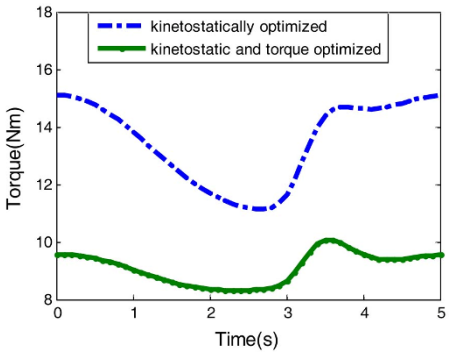


(a) Torque at joint 1

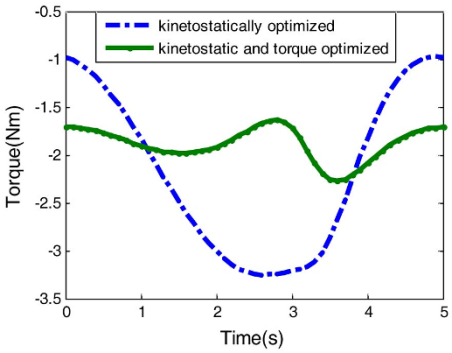


(b) Torque at joint 2

Fig. 2. Comparison of torques before and after torque optimization.

the two-DOF planar arm whose link lengths were chosen on the basis of kinetostatic optimization [9]. Effect of dynamics on this robot is not discussed in Ref. [9]. Hence, the torque optimization based on the mass distribution presented in this section is a valuable contribution towards a suitably optimized design of a two-link two-DOF robot arm from both kinematic and dynamic points of view.

### *4.1 A Kinetostatically optimized robot*

The design of a two-link robot arm based on the kinetostatic optimization, as given in Ref. [9], suggests the link lengths as a $a_2 : a_1 = \sqrt{2} : 2$ . It leads to the unity condition number of the Jacobian given by Eq. (4). Note that the unity condition number of the Jacobian is satisfied as when $\theta_1 = 0$ and $\theta_2 = 3\pi/4$. Hence, a trajectory around this configuration will provide the best kinematic performance.

### *4.2 Objective function*

The objective of optimization here is to find the robot's dynamic parameters for which the joint torques are minimized. For this, the weighted sum of the root mean squares (RMS) of the joint torques are minimized. Out of several criteria, the RMS is chosen for the reason that it gives equal emphasis on the results at every time instance [13].

The weights $w_i$'s were chosen such that the sum is equal to one [16]: $\sum w_i = 1$ . The optimality criterion is proposed here as

$$\text{Minimize} \quad z(\mathbf{x}) = w_1 \tau_{1,rms} + w_2 \tau_{2,rms} \,. \tag{24}$$

### *4.3 Design variables and constraints*

A joint torque is influenced by link inertias, namely, the link masses and the moment of inertia. These inertia properties are conveniently represented by point-masses. Accordingly, the design variables are defined as

$$\mathbf{x} \equiv [m_{11}, m_{12}, m_{13}, r_{11}, m_{21}, m_{22}, m_{23}, r_{21}]^T \,. \tag{25}$$

The constraints should be implicit or the explicit function of design variables, and to be bound in such a way that the practical design solution is obtained. Here, the inequality constraints are also considered. The important condition of practical solution is that the moment of inertia of each link about its center of mass must be positive. The negative values of point-masses do not matter till the total mass of the link is positive and moment of inertia about the center of mass is also positive. Besides, the location of the center of mass must not be too far.

These constraints, for $i = 1,2$, and $j = 1,2,3$, are listed below:

$$m_i^o \le \sum_{j=1}^{3} m_{ij} \le 1.1 m_i^o \quad , \tag{26a}$$

$$m_i r_i^2 \le (I_i - \Delta) \,, \tag{26b}$$

$$0.5 r_{ij}^o \le r_{ij} \le 1.5 r_{ij}^o \,, \tag{26c}$$

where $m_i^o$ and $r_{ij}^o$ are the parameters related to the original robot. Here, original refers to the robot parameters before optimization. Note in Eq. (26b), $\Delta$ is very small such that $m_i r_i^2 < I_i$ . The 'fmincon' function of MATLAB's [18] optimization tool box was used to minimize the multi-variable function z given by Eq. (24).

### *4.4 Numerical example*

The parameters of the two-DOF robot are shown in Table 1. The joint trajectories were calculated, as given in sub-Sec. 3.2 for the circular end-effector trajectory. The circle's center is at $u$ (0.5858 m) and $v$ (0.5858 m) whose radius $l$ = 0.3 m. The motion was to be completed in 5 seconds. The location of circular trajectory was chosen such that the pose of the kinetostatic optimized robot does not deflect much from its pose of condition number one [9]. The robot's equivalent point-masses are also given in Table 1.

## 5. Results and discussion

For the weighing factors ($w_1$, $w_2$) = (0.5, 0.5), both for the robot were analyzed. One can change weights and see their

Table 1. Mass and inertia properties of the kinetostatically optimized robot.

| | | Link parameters | | | Three point-mass model | | | | |
|---|---|---|---|---|---|---|---|---|---|
| Link ($i$) | $m_i$ ($kg$) | $a_i$ ($m$) | $r_i$ ($m$) | $\psi_i$ ($deg$) | $I_i^c$ ($kg$-$m^2$) | $m_{i1}$ ($kg$) | $m_{i2}$ ($kg$) | $m_{i3}$ ($kg$) | $r_{i1}$ ($m$) |
| 1 | 1.1715 | 1.1715 | 0.5857 | 180 | 0.1339 | -0.2859 | 0.7287 | 0.7287 | 0.6764 |
| 2 | 0.8285 | 0.8285 | 0.4142 | 180 | 0.0473 | -0.2021 | 0.5153 | 0.5153 | 0.4783 |

Table 2. Mass and inertia properties of the kinetostatically optimized robot after torque optimization.

| | | | Link parameters | | | Three point-mass model | | | | |
|---|---|---|---|---|---|---|---|---|---|---|
| ($w_1$ , $w_2$) | Link ($i$) | $m_i$ ($kg$) | $a_i$ ($m$) | $r_i$ ($m$) | $\psi_i$ ($deg$) | $I_i^c$ ($kg$-$m^2$) | $m_{i1}$ ($kg$) | $m_{i2}$ ($kg$) | $m_{i3}$ ($kg$) | $r_{i1}$ ($m$) |
| (0.5 , 0.5) | 1 | 1.1715 | 1.1715 | 1.0095 | 178.98 | 0.0103 | -0.3865 | 0.7909 | 0.7671 | 1.0146 |
| | 2 | 0.8284 | 0.8284 | 0.6534 | 166.02 | 0.0073 | -0.2553 | 0.6564 | 0.4273 | 0.6589 |

Table 3. RMS values of the torques.

| Type, ($w_1$ , $w_2$) | $\tau_{1,rms}$ | $\tau_{2,rms}$ |
|---|---|---|
| Kinetostatically optimized robot | 13.58 | 2.32 |
| Kinetostatic and torque optimized robot, (0.5 , 0.5) | 9.12 (**-32.84**)* | 1.88 (**-18.96**) |

* The values in parenthesis indicate the percentage reduction from original value.

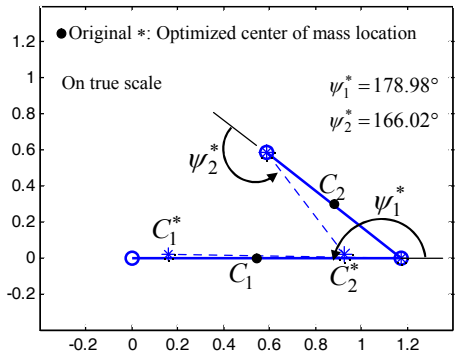


Fig. 3. Locations of the optimized centers of masses.

effects on the results by rerunning the MATLAB program written for the purpose. However, selection of weights depends on how critical the designed parameters would be. For example, if the user does not want to make the 2nd motor large, more weight is to be given to it to make its torque requirement less, hence, the size and weight. In Ref. [17] the effect of weights on balancing of mechanism was well studied. Table 2 shows the optimized design variables and the corresponding change in the original link parameters, namely, the mass, mass center location, and moment of inertia. The changed parameters have been calculated using the values of optimized design variables substituted in equimomental conditions. For the equimomental conditions refer Ref. [13]. The RMS values of the torques are given in Table 3.

## 6. Conclusions

This paper has presented the dynamics formulation using the equimomental system of point-masses and its application to optimization of joint torques by redistributing the link masses. The three point-mass equimomental system was used to replace a rigid body. Equations of motion in point-masses were derived recursively to obtain the joint torques using Newton's equations of linear motion and the corresponding DeNOC matrices for the point-masses. The proposed methodology was implemented to compare the performance of the kinetostatic optimized robot with the torque optimization. As a result, a complete optimization, from both kinematic and dynamic points of view, was undertaken, which is expected to certainly provide an improved robot design than only kinetostatically optimized robot arm.

## Acknowledgment

The financial support given to the first author from the project entitled "Design and Development of Mathematical Model based 6-DOF Electrical Motion Platform," sponsored by the Simulator Development Division, Secunderabad, is duly acknowledged.

## References

[1] M. Husain, A. K. Mallik and A. Ghosh, Design improvement of manipulators by minimizing shaking force/moment and driving torques, *ASME Mechanism Conference, Tempe*, AZ, DE (1992) 139-147.

[2] H. C. Chou and J. P. Sadler, Optimal location of robot trajectories for minimization of actuator torque, *Mechanisms and Machine Theory*, 28 (1993) 145-158.

[3] D. F. Berner and J. A. Snyman, The influence of joint angle constraints on the optimum design of a planar robot manipulator following a complicated prescribed path, *Computers and Mathematics with Applications,* 37 (1999) 111-124.

[4] J. A. Snyman and D. F. Berner, A mathematical optimiza-

tion methodology for the optimal design of a planar robotic manipulator, *International J. for Numerical Methods in Engineering*, 44 (1999) 535-550.
[5] J. A. Snyman and F. V. Tonder, Optimum design of a three-dimensional serial robot manipulator, *Structural Optimization*, 17 (1999) 172-185.
[6] V. Arakelian, J. L. Baron and P. Mottu, Torque minimization of the 2-DOF serial manipulators based on minimum energy consideration and optimum mass redistribution, *Mechatronics*, 21 (2011) 310-314.
[7] H. Diken, Effect of mass balancing on the actuator torques of a manipulator, *Mechanism Machine Theory*, 30 (1995) 495-500.
[8] H. Chaudhary and S. K. Saha, Minimization of constraint forces in industrial manipulator, *IEEE International Conference on Robotics and Automation*, Italy (2007) 1954-195.
[9] W. A. Khan and J. Angeles, The kinetostatic optimization of robotic manipulators: The inverse and the direct problem, *ASME J. of Mechanical Design*, 128 (2006) 168-178.
[10] S. K. Saha, Dynamics of serial multibody systems using the decoupled natural orthogonal complement matrices, *Transaction of ASME*, 66 (1999) 986-996.
[11] V. Gupta, S. K. Saha and H. Chaudhary, Dynamics of serial-chain multibody systems using equimomental systems of point-masses, *Multibody Dynamics, ECCOMAS Thematic Conference*, Croatia (2013) 741-749.
[12] E. J. Routh, *Treatise on the dynamics of a system of rigid bodies, Elementary Part-I*, Dover publication Inc., New York (1905).
[13] H. Chaudhary and S. K. Saha, *Dynamics and balancing of multibody systems*, Springer, Berlin (2009).
[14] K. Chaudhary and H. Chaudhary, Dynamic balancing of planar mechanisms using genetic algorithm, *JMST*, 28 (10) (2014) 4213-4220.
[15] S. K. Saha, *Introduction to robotics*, Tata McGraw Hill, New Delhi (2008).
[16] R. T. Marler and J. S. Arora, The weighted sum method for multi-objective optimization: new insights, *Struct Multidisc Optim*, 41 (2010) 853-862.
[17] S. Erkaya, Investigation of balancing problem for a planar mechanism using genetic algorithm, *JMST*, 27 (7) (2013) 2153-2160.
[18] *MATLAB*: *Optimization Toolbox*, Version R2013a.

**Vinay Gupta** received his B.E. in Mechanical Engineering from Dr. B. R. A. University Agra in 2000 and M.Tech from UPTU Lucknow in 2009. He is currently a Ph.D. student in Mechanical Engineering at Indian Institute of Technology Delhi, New Delhi, India.

**Himanshu Chaudhary** is an associate professor in Mechanical Engineering at Malaviya National Institute of Technology Jaipur, India. His research areas are multibody dynamics, dynamic balancing and optimization of mechanisms including robotic systems.

**Subir K. Saha** is a professor in Mechanical Engineering at Indian Institute of Technology Delhi, New Delhi India. His research areas are robotics and mechanisms & multibody dynamics.